

Original citation:

LHCb Collaboration (Including: Back, John J., Craik, Daniel, Dossett, D., Gershon, Timothy J., Kreps, Michal, Latham, Thomas, Pilar, T., Poluektov, Anton, Reid, Matthew M., Silva Coutinho, R., Whitehead, M. (Mark) and Williams, Matthew P.). (2013) Search for direct CP violation in $D^0 \rightarrow h^- h^+$ modes using semileptonic B decays. Physical Letters B, Volume 723 (Number 1-3). pp. 33-43. ISSN 1098-0121

Permanent WRAP url:

<http://wrap.warwick.ac.uk/58797>

Copyright and reuse:

The Warwick Research Archive Portal (WRAP) makes this work of researchers of the University of Warwick available open access under the following conditions.

This article is made available under the Creative Commons Attribution 3.0 (CC BY 3.0) license and may be reused according to the conditions of the license. For more details see: <http://creativecommons.org/licenses/by/3.0/>

A note on versions:

The version presented in WRAP is the published version, or, version of record, and may be cited as it appears here.

For more information, please contact the WRAP Team at: publications@warwick.ac.uk



<http://wrap.warwick.ac.uk>



Search for direct CP violation in $D^0 \rightarrow h^- h^+$ modes using semileptonic B decays[☆]

LHCb Collaboration

ARTICLE INFO

Article history:

Received 13 March 2013
 Received in revised form 18 April 2013
 Accepted 29 April 2013
 Available online 3 May 2013
 Editor: L. Rolandi

ABSTRACT

A search for direct CP violation in $D^0 \rightarrow h^- h^+$ (where $h = K$ or π) is presented using data corresponding to an integrated luminosity of 1.0 fb^{-1} collected in 2011 by LHCb in pp collisions at a centre-of-mass energy of 7 TeV. The analysis uses D^0 mesons produced in inclusive semileptonic b -hadron decays to the $D^0 \mu X$ final state, where the charge of the accompanying muon is used to tag the flavour of the D^0 meson. The difference in the CP -violating asymmetries between the two decay channels is measured to be

$$\Delta A_{CP} = A_{CP}(K^- K^+) - A_{CP}(\pi^- \pi^+) = (0.49 \pm 0.30 \text{ (stat)} \pm 0.14 \text{ (syst)})\%.$$

This result does not confirm the evidence for direct CP violation in the charm sector reported in other analyses.

© 2013 CERN. Published by Elsevier B.V. All rights reserved.

1. Introduction

The combined symmetry of charge conjugation and parity (CP) is broken in the weak interaction of the Standard Model by a single phase in the Cabibbo–Kobayashi–Maskawa matrix [1,2]. Physics beyond the Standard Model may reveal itself in the form of additional sources of CP violation. In both the K^0 and B^0 systems CP violation has been unambiguously observed, and is in agreement with the Standard Model predictions. In contrast, CP violation in the charm sector has yet to be established. The amount of CP violation in charm decays was generally expected to be much smaller than the 1% level in the Standard Model [3,4]. The LHCb collaboration, however, reported evidence with 3.5 standard deviations significance for direct CP violation in two-body, singly-Cabibbo-suppressed D^0 decays [5]. The difference in CP asymmetries between $D^0 \rightarrow K^- K^+$ and $D^0 \rightarrow \pi^- \pi^+$ decays was found to be $\Delta A_{CP} = (-0.82 \pm 0.21 \text{ (stat)} \pm 0.11 \text{ (syst)})\%$. This result sparked a theoretical debate on whether or not this could be accommodated within the Standard Model. For a comprehensive review see Ref. [6].

After the LHCb paper, the CDF and Belle collaborations presented measurements of $\Delta A_{CP} = (-0.62 \pm 0.21 \text{ (stat)} \pm 0.10 \text{ (syst)})\%$ [7] and $\Delta A_{CP} = (-0.87 \pm 0.41 \text{ (stat)} \pm 0.06 \text{ (syst)})\%$ [8], respectively. These numbers are included in the average from the Heavy Flavor Averaging Group (HFAG) [9], together with a previous measurement [10] from the BaBar collaboration, yield-

ing a world average of the difference in direct CP violation of $\Delta a_{CP}^{\text{dir}} = (-0.68 \pm 0.15)\%$.¹

In all previous results $D^{*+} \rightarrow D^0 \pi^+$ decays² have been used as the source of the D^0 sample, and the emitted pion was used to determine the flavour of the neutral D meson (i.e., whether it is D^0 or \bar{D}^0). In this Letter a measurement of ΔA_{CP} is presented using D^0 mesons produced in semileptonic b -hadron decays where the flavour of the neutral D meson is tagged by the accompanying charged lepton. This approach provides an independent determination of ΔA_{CP} .

2. Method and formalism

The measured (raw) asymmetry for a D^0 decay to a CP eigenstate f is defined as

$$A_{\text{raw}} = \frac{N(D^0 \rightarrow f) - N(\bar{D}^0 \rightarrow f)}{N(D^0 \rightarrow f) + N(\bar{D}^0 \rightarrow f)}, \quad (1)$$

where N denotes the observed yield for the given decay. The initial flavour of the neutral D meson is tagged by the charge of the accompanying muon in the semileptonic b -hadron (B) decay to the $D \mu X$ final state. A positive muon is associated with a \bar{D}^0 meson, and a negative muon with a D^0 meson. The X denotes any other particle(s) produced in the semileptonic B decay, which are not reconstructed (e.g., the neutrino).

¹ The relation between ΔA_{CP} and $\Delta a_{CP}^{\text{dir}}$ is explained in Section 6.

² The inclusion of charge-conjugated modes is implied throughout this Letter, unless explicitly stated otherwise.

[☆] © CERN for the benefit of the LHCb Collaboration.

The raw asymmetry can be written in terms of the D^0 decay rate, Γ , the muon detection efficiency, ε , and the D^0 production rate in semileptonic b -hadron decays, \mathcal{P} , as

$$A_{\text{raw}} = \frac{\Gamma(D^0)\varepsilon(\mu^-)\mathcal{P}(D^0) - \Gamma(\bar{D}^0)\varepsilon(\mu^+)\mathcal{P}(\bar{D}^0)}{\Gamma(D^0)\varepsilon(\mu^-)\mathcal{P}(D^0) + \Gamma(\bar{D}^0)\varepsilon(\mu^+)\mathcal{P}(\bar{D}^0)}. \quad (2)$$

Defining the CP asymmetry as $A_{CP} = (\Gamma(D^0) - \Gamma(\bar{D}^0))/(\Gamma(D^0) + \Gamma(\bar{D}^0))$, the muon detection asymmetry as $A_D^\mu = (\varepsilon(\mu^-) - \varepsilon(\mu^+))/(\varepsilon(\mu^-) + \varepsilon(\mu^+))$, and the effective production asymmetry as $A_P^B = (\mathcal{P}(D^0) - \mathcal{P}(\bar{D}^0))/(\mathcal{P}(D^0) + \mathcal{P}(\bar{D}^0))$, the raw asymmetry can be written to first order as

$$A_{\text{raw}} \approx A_{CP} + A_D^\mu + A_P^B. \quad (3)$$

The effective production asymmetry is due to different production rates of b - and \bar{b} -hadrons and also includes any effect due to semileptonic asymmetries in neutral B mesons. As the detection and production asymmetries are of order 1%, the approximation in Eq. (3) is valid up to corrections of order 10^{-6} . Both detection and production asymmetries differ from those in the analyses using $D^{*\pm}$ decays, where the $D^{*\pm}$ mesons are produced directly in the primary pp interaction. In these ‘‘prompt’’ decays a possible detection asymmetry enters through the reconstruction of the tagging pion, and the production asymmetry is that of the prompt $D^{*\pm}$ mesons.

By taking the difference between the raw asymmetries measured in the $D^0 \rightarrow K^-K^+$ and $D^0 \rightarrow \pi^-\pi^+$ decays the detection and production asymmetries cancel, giving a robust measurement of the CP asymmetry difference

$$\begin{aligned} \Delta A_{CP} &= A_{\text{raw}}(K^-K^+) - A_{\text{raw}}(\pi^-\pi^+) \\ &\approx A_{CP}(K^-K^+) - A_{CP}(\pi^-\pi^+). \end{aligned} \quad (4)$$

Since the detection and the production depend on the kinematics of the process under study, the cancellation is only complete when the kinematic distributions of the muon and b -hadron are the same for both $D^0 \rightarrow K^-K^+$ and $D^0 \rightarrow \pi^-\pi^+$. A weighting procedure is used to improve the cancellation by equalising the kinematic distributions.

3. Detector and simulation

The LHCb detector [11] is a single-arm forward spectrometer covering the pseudorapidity range $2 < \eta < 5$, designed for the study of particles containing b or c quarks. The detector includes a high-precision tracking system consisting of a silicon-strip vertex detector surrounding the pp interaction region, a large-area silicon-strip detector located upstream of a dipole magnet with a bending power of about 4 Tm, and three stations of silicon-strip detectors and straw drift tubes placed downstream. The polarity of the magnet is reversed repeatedly during data taking, which causes all detection asymmetries that are induced by the left-right separation of charged particles to change sign. The combined tracking system has momentum resolution $\Delta p/p$ that varies from 0.4% at 5 GeV/c to 0.6% at 100 GeV/c, and impact parameter resolution of 20 μm for tracks with high transverse momentum. Charged hadrons are identified using two ring-imaging Cherenkov detectors [12]. Muons are identified by a system composed of alternating layers of iron and multiwire proportional chambers. The trigger [13] consists of a hardware stage, based on information from the calorimeter and muon systems, followed by a software stage, which applies a full event reconstruction.

In the simulation, pp collisions are generated using PYTHIA 6.4 [14] with a specific LHCb configuration [15]. Decays of hadronic

particles are described by EVTGEN [16] in which final state radiation is generated using PHOTOS [17]. The interaction of the generated particles with the detector and its response are implemented using the GEANT4 toolkit [18] as described in Ref. [19]. The B^+ and B^0 mesons in the simulated events are forced to decay semileptonically using a cocktail of decay modes, including those that involve excited D states and τ leptons, that lead to final states with a D^0 meson and a muon.

4. Data set and selection

This analysis uses the LHCb 2011 data set, corresponding to an integrated luminosity of 1.0 fb^{-1} , of which 0.4 fb^{-1} is taken with the magnet field pointing up and 0.6 fb^{-1} with the magnet field pointing down. The measurement of ΔA_{CP} is performed separately for the two field polarities. The final value for ΔA_{CP} is obtained by taking the arithmetic mean of the two results to reduce as much as possible any residual effect of the detection asymmetry. To minimise potential trigger biases the candidates are required to be accepted by specific trigger decisions. About 87% of the candidates in the final selection are triggered at the hardware stage by the muon system only, about 3% by the hadronic calorimeter only and about 10% by both. The muon trigger requires the muon transverse momentum, p_T , to be greater than 1.48 GeV/c. The effect of a charge-dependent shift in the p_T estimate in this trigger is corrected, which requires tightening the muon transverse momentum cut, as measured by the hardware trigger, to $p_T > 1.64 \text{ GeV/c}$. In the software trigger the candidates are selected by either a single muon trigger or by a topological trigger, which selects combinations of a muon with one or two additional tracks that are consistent with the topological signature of b -hadron decays. At this level, 5% of the candidates in the final selection are selected by the single muon trigger only, 79% by the topological trigger only, and 16% by both.

In order to suppress backgrounds, the χ^2 per degree of freedom of the track fit is required to be smaller than 4 for the kaons and pions and smaller than 5 for the muon. Furthermore, the χ^2 per degree of freedom of each of the b -hadron and D^0 decay vertex fits is required to be smaller than 6, and the impact parameter χ^2 (defined as the difference between the χ^2 of the primary vertex formed with and without the considered tracks) is required to be larger than 9 for all three tracks. The significance of the distance between the primary vertex and the D^0 decay vertex is required to be above 10. The momentum and transverse momentum of the muon are required to be above 3 GeV/c and 1.2 GeV/c,³ and the momentum and transverse momentum of the D^0 daughters above 2 GeV/c and 0.3 GeV/c. The D^0 transverse momentum must be above 0.5 GeV/c and the scalar p_T sum of its daughters above 1.4 GeV/c. The invariant mass of the D^0 -muon combination is required to be between 2.5 and 5.0 GeV/c² to suppress background. The upper bound removes three-body final state b -hadron decays. The reconstructed decay time of the D^0 meson (measured from the b -hadron decay vertex) is required to be positive. The requirement on the muon impact parameter reduces the contribution from D^0 mesons produced directly in the pp collision to below 3%. Requirements on the D^0 decay topology are minimal in order to keep the lifetime acceptance similar for the $D^0 \rightarrow K^-K^+$ and $D^0 \rightarrow \pi^-\pi^+$ modes.

A potentially significant background from $B \rightarrow J/\psi X$ decays is suppressed by removing candidates where the invariant mass of the muon and the oppositely-charged D^0 daughter is within

³ This cut affects mainly the candidates triggered by the hadronic calorimeter at the hardware level.

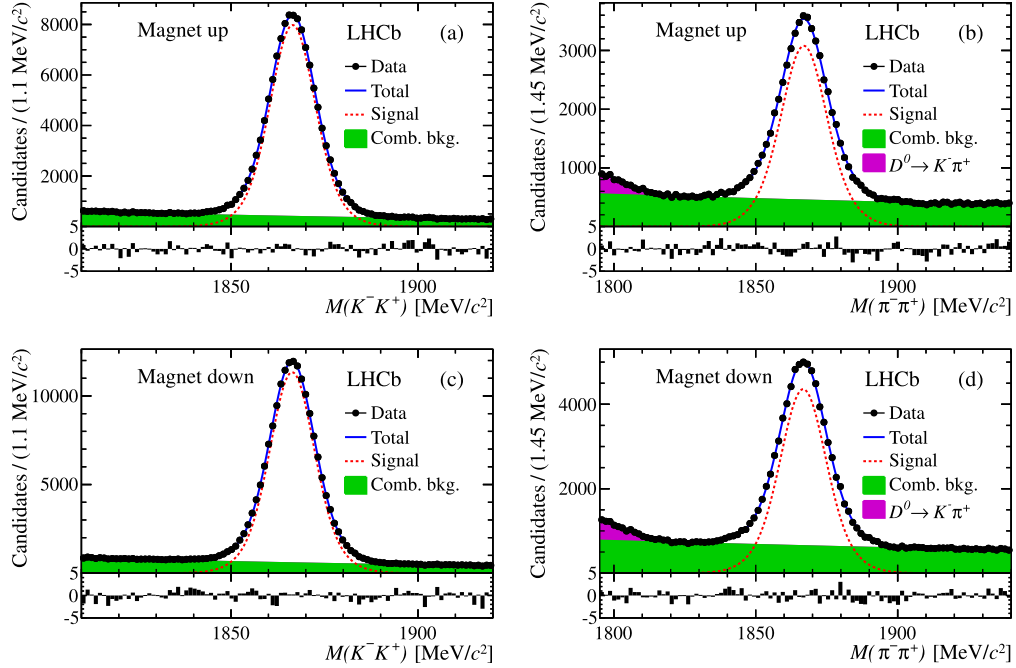


Fig. 1. Invariant mass distributions for (a, c) $D^0 \rightarrow K^-K^+$ and (b, d) $D^0 \rightarrow \pi^-\pi^+$ muon-tagged candidates for the two magnet polarities. The result of the fit is overlaid, showing the contribution from signal, combinatorial background and $D^0 \rightarrow K^-\pi^+$ reflection. Underneath each plot the pull in each mass bin is shown.

three times the mass resolution from the J/ψ or $\psi(2S)$ mass and the D^0 daughter passes muon identification requirements. Reflections from Cabibbo-favoured $D^0 \rightarrow K^-\pi^+$ decays are observed in the mass regions below and above the signal peaks in the $D^0 \rightarrow \pi^-\pi^+$ and $D^0 \rightarrow K^-K^+$ samples, respectively. Information from the relevant detectors in LHCb is combined into differences between the logarithms of the particle identification likelihoods under different mass hypotheses (DLL). The selected kaons are required to have $\text{DLL}_{K\pi} \equiv \ln \mathcal{L}_K - \ln \mathcal{L}_\pi > 10$ and the selected pions are required to have $\text{DLL}_{K\pi} < -2$. The $D^0 \rightarrow K^-\pi^+$ mode is used as a control channel and is selected with the same requirements as the two decay modes of interest.

5. Determination of the asymmetries

The invariant mass distributions for the muon-tagged D^0 candidates are shown in Fig. 1. To determine the numbers of signal candidates after selection, a binned maximum likelihood fit to each of these distributions is performed. The signal is modelled by the sum of two Gaussian functions with common means, but different widths. The combinatorial background is described by an exponential shape. For the $\pi^-\pi^+$ invariant mass distribution the fit is performed in the range between 1795 and 1940 MeV/c^2 and a Gaussian distribution is used to model the tail of the reflection from $D^0 \rightarrow K^-\pi^+$ decays. For the K^-K^+ invariant mass distribution the fit range is restricted to 1810–1920 MeV/c^2 such that the contamination from the $D^0 \rightarrow K^-\pi^+$ reflection and from partially reconstructed $D^0 \rightarrow K^-K^+\pi^0$ and $D^+ \rightarrow K^-K^+\pi^+$ decays is negligible. The total number of signal candidates determined from the fit is $(558.9 \pm 0.9) \times 10^3$ for $D^0 \rightarrow K^-K^+$ decays and $(221.6 \pm 0.8) \times 10^3$ for $D^0 \rightarrow \pi^-\pi^+$ decays.

The raw asymmetries are determined with simultaneous binned likelihood fits to the D^0 mass distributions for positive and negative muon tags where the shape parameters for the signal and the $D^0 \rightarrow K^-\pi^+$ reflection are required to be the same. The back-

Table 1

Unweighted raw asymmetries (in %) for the $D^0 \rightarrow \pi^-\pi^+$, $D^0 \rightarrow K^-K^+$ and $D^0 \rightarrow K^-\pi^+$ decays for the two magnet polarities. The mean value is the arithmetic average over the two polarities. The uncertainties are statistical only.

	Magnet up	Magnet down	Mean
$A_{\text{raw}}^{\text{unweighted}}(K^-K^+)$	-0.33 ± 0.23	-0.22 ± 0.19	-0.28 ± 0.15
$A_{\text{raw}}^{\text{unweighted}}(\pi^-\pi^+)$	-1.18 ± 0.40	-0.35 ± 0.34	-0.77 ± 0.26
$\Delta A_{\text{CP}}^{\text{unweighted}}$	0.85 ± 0.46	0.13 ± 0.39	0.49 ± 0.30
$A_{\text{raw}}^{\text{unweighted}}(K^-\pi^+)$	-1.64 ± 0.10	-1.60 ± 0.08	-1.62 ± 0.06

ground shape can vary independently for positive and negative muon tags. Table 1 lists the raw asymmetries for both modes, and for the $D^0 \rightarrow K^-\pi^+$ control mode. An additional asymmetry in the $D^0 \rightarrow K^-\pi^+$ mode originates from the different cross-sections in matter for positive and negative kaons. It can be seen that the asymmetry in this mode is consistent for the two magnetic field polarities, which indicates that the detection asymmetry related to the magnetic field is at most $\mathcal{O}(10^{-3})$.

5.1. Differences in kinematic distributions

Since the detection and production asymmetries may have kinematic dependences, the cancellation in Eq. (4) is only valid if the kinematic distributions of the muon and b -hadron are similar for both $D^0 \rightarrow K^-K^+$ and $D^0 \rightarrow \pi^-\pi^+$ decays. After the trigger and selection requirements the kinematic distributions for the two decay modes are, however, slightly different. Although the selection is largely the same, the particle identification requirements introduce differences in the momentum distributions. In addition, due to the difference in available phase space, the pions in $D^0 \rightarrow \pi^-\pi^+$ decays have a harder momentum spectrum compared to the kaons in $D^0 \rightarrow K^-K^+$ decays. The muon trigger and selection requirements are identical. Nevertheless, the D^0 meson and the muon are kinematically correlated since they originate from the same decay, causing also the muon kinematic distribu-

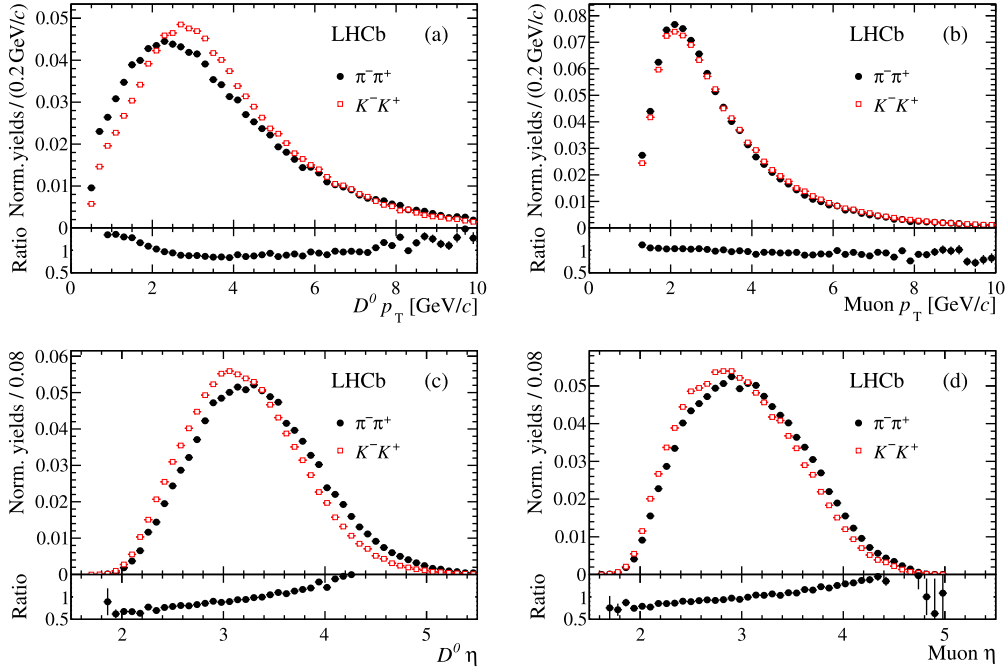


Fig. 2. Kinematic distributions of the (a, c) D^0 meson and (b, d) muon for $D^0 \rightarrow \pi^- \pi^+$ (black circles) and $D^0 \rightarrow K^- K^+$ (red squares) candidates normalised to unit area. The histograms show the distributions of signal candidates, after background subtraction. Underneath each plot the ratio of the two distributions is shown.

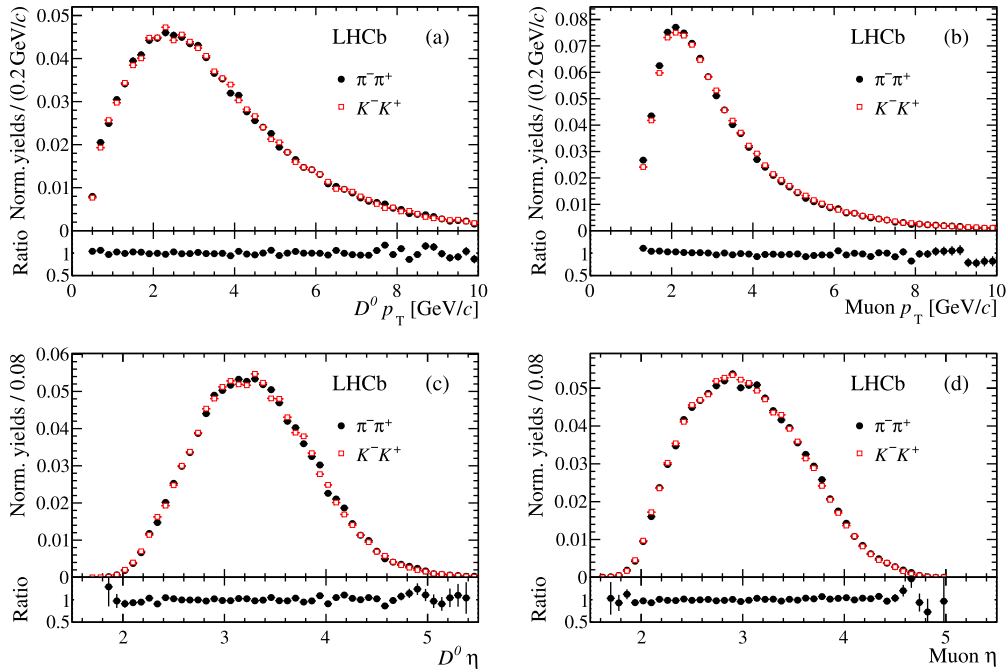


Fig. 3. Kinematic distributions of the (a, c) D^0 meson and (b, d) muon for $D^0 \rightarrow \pi^- \pi^+$ (black circles) and $D^0 \rightarrow K^- K^+$ (red squares) candidates normalised to unit area after the weighting procedure. The histograms show the distributions of signal candidates, after background subtraction. Underneath each plot the ratio of the two distributions is shown.

tions to be different for the two decay modes. Fig. 2 shows the p_T and pseudorapidity η distributions for the D^0 meson and the muon. The background has been statistically subtracted using the *sPlot* method [20]. In order to obtain the same kinematic distributions for both decays, the D^0 candidates are given a weight depending on their p_T and η values. The weights are obtained from a comparison of the background-subtracted distributions and are applied to either $D^0 \rightarrow K^- K^+$ or $D^0 \rightarrow \pi^- \pi^+$ candidates depending on which has most events in the given kinematic bin. Fig. 3

shows the weighted kinematic distributions for both decay modes. Whereas the weights are determined purely on the basis of the $D^0 p_T$ and η distributions, after the weighting, the muon distributions are also in excellent agreement. The raw asymmetries after the weighting procedure for the $D^0 \rightarrow K^- K^+$ and $D^0 \rightarrow \pi^- \pi^+$ modes are given in Table 2. There are minor changes in the values of the raw asymmetries and ΔA_{CP} with respect to the unweighted results, showing that the effect of the difference in kinematic distributions is small.

Table 2

Weighted raw asymmetries (in %) for the $D^0 \rightarrow \pi^- \pi^+$ and $D^0 \rightarrow K^- K^+$ decays for the two magnet polarities. The mean value is the arithmetic average over the two polarities. The uncertainties are statistical only.

	Magnet up	Magnet down	Mean
$A_{\text{raw}}(K^- K^+)$	-0.39 ± 0.23	-0.20 ± 0.19	-0.29 ± 0.15
$A_{\text{raw}}(\pi^- \pi^+)$	-1.25 ± 0.40	-0.29 ± 0.34	-0.77 ± 0.26
ΔA_{CP}	0.86 ± 0.46	0.09 ± 0.39	0.48 ± 0.30

5.2. Wrong flavour tags

In some cases the D^0 flavour is not tagged correctly by the muon charge due to misreconstruction (e.g., a prompt D^0 decay can be combined with a random muon). The probability to tag a D^0 meson with a positive muon is denoted by ω^+ and the probability to tag a \bar{D}^0 meson with a negative muon by ω^- . The average mistag probability is $\bar{\omega} = (\omega^+ + \omega^-)/2$ and the mistag difference is $\Delta\omega = \omega^+ - \omega^-$. The raw asymmetry in Eq. (3) is then modified to

$$A_{\text{raw}} \approx (1 - 2\bar{\omega})(A_{CP} + A_D^{\mu} + A_p^{\beta}) - \Delta\omega, \quad (5)$$

which makes clear that the average mistag probability dilutes the observed asymmetry, while any difference in the mistag probability for D^0 and \bar{D}^0 gives rise to a systematic shift in A_{raw} . Assuming that the values of $\bar{\omega}$ and $\Delta\omega$ are the same for $D^0 \rightarrow K^- K^+$ and $D^0 \rightarrow \pi^- \pi^+$, the value of ΔA_{CP} is then corrected as

$$\Delta A_{CP} = (1 - 2\bar{\omega})^{-1}(A_{\text{raw}}(K^- K^+) - A_{\text{raw}}(\pi^- \pi^+)). \quad (6)$$

The mistag probability is estimated from the $D^0 \rightarrow K^- \pi^+$ sample. As the $D^0 \rightarrow K^- \pi^+$ decay is almost self-tagging the mistag probability is determined using the charge of the final state (either $K^+ \pi^-$ or $K^- \pi^+$). The wrongly tagged decays include a fraction of doubly-Cabibbo-suppressed $D^0 \rightarrow K^+ \pi^-$ and mixed $D^0 \rightarrow \bar{D}^- \rightarrow K^+ \pi^-$ decays. This fraction is calculated to be $(0.393 \pm 0.007)\%$ using input from Ref. [21]. After correcting for this fraction the average mistag probability, $\bar{\omega}$, is found to be $(0.982 \pm 0.012)\%$, which means that the effect from wrong tags constitutes only a small correction on the observed asymmetries. This number also provides an upper bound of about 2% from any background from real D^0 decays with a random muon, which includes promptly produced D^0 decays. The difference in mistag probabilities for D^0 and \bar{D}^0 mesons is found to be $\Delta\omega = (0.006 \pm 0.021)\%$ and is neglected.

As a cross-check the mistag probabilities are also determined from a doubly-tagged sample by reconstructing $B \rightarrow D^{*+} \mu^- X$ decays where the D^{*+} decays to $D^0 \pi^+$ and comparing the charge of the pion with that of the muon. The fraction of wrongly tagged decays is estimated from a simultaneous fit, similar to that in Ref. [22], to the distribution of $\Delta M = M(h^- h^+ \pi^+) - M(h^- h^+)$ for the full sample and for the wrongly tagged decays. The mistag probability in the $D^0 \rightarrow K^- \pi^+$ sample is $(0.880 \pm 0.043)\%$, while the average mistag probability in the $D^0 \rightarrow K^- K^+$ and $D^0 \rightarrow \pi^- \pi^+$ samples equals $(1.00 \pm 0.09)\%$. The largest difference with the result obtained from the full $D^0 \rightarrow K^- \pi^+$ sample (i.e., 0.102%) is assigned as a systematic uncertainty in the mistag probability. The difference in mistag probabilities, $\Delta\omega$, in this cross-check is also consistent with zero.

After the weighting and correcting for the mistag probability of $(0.982 \pm 0.012(\text{stat}) \pm 0.102(\text{syst}))\%$, the difference of the raw asymmetries between the two modes is found to be

$$\Delta A_{CP} = (0.49 \pm 0.30)\%,$$

where the uncertainty is statistical only. The corresponding systematic uncertainties are discussed in Section 7.

6. Measurement of the average decay times

The time-integrated asymmetry for a decay to a CP eigenstate f is defined as

$$A_{CP} = \frac{\Gamma(D^0 \rightarrow f) - \Gamma(\bar{D}^0 \rightarrow f)}{\Gamma(D^0 \rightarrow f) + \Gamma(\bar{D}^0 \rightarrow f)}, \quad (7)$$

where Γ is the decay rate for the given channel. As the reconstruction and selection requirements for the two decay modes are not identical, the decay time acceptance can be different. This introduces a difference in the contribution from direct and indirect CP violation for the two modes. When assuming the CP violating phase in D^0 oscillations, ϕ , to be universal [4], the difference between the asymmetries for $D^0 \rightarrow K^- K^+$ and $D^0 \rightarrow \pi^- \pi^+$ can be written in terms of direct and indirect CP violation as [23]

$$\Delta A_{CP} \approx \Delta a_{CP}^{\text{dir}} \left(1 + y \frac{\langle \bar{t} \rangle}{\tau} \cos \phi \right) + (a_{CP}^{\text{ind}} + \bar{a}_{CP}^{\text{dir}} y \cos \phi) \frac{\Delta \langle t \rangle}{\tau}. \quad (8)$$

In this equation the indirect CP violation is $a_{CP}^{\text{ind}} = -(A_m/2)y \cos \phi + x \sin \phi$, x and y are the D^0 mixing parameters, A_m represents the CP violation from mixing, τ is the average D^0 lifetime, $\Delta a_{CP}^{\text{dir}}$ and $\bar{a}_{CP}^{\text{dir}}$ are the direct CP violation difference and average of the two decay modes, and $\Delta \langle t \rangle$ and $\langle \bar{t} \rangle$ are the difference and average of the two mean decay times. Under SU(3) flavour symmetry, the direct asymmetries in the individual modes are expected to have opposite sign and therefore add constructively in the difference. Furthermore, since y is of order 1%, $\langle \bar{t} \rangle/\tau$ is $\mathcal{O}(1)$ and $\Delta \langle t \rangle/\tau$ is close to zero, ΔA_{CP} is essentially equal to the difference in direct CP violation, $\Delta a_{CP}^{\text{dir}}$. While y and $\cos \phi$ can be obtained from the HFAG averages [9], in order to interpret ΔA_{CP} in terms of direct and indirect CP violation, the mean decay time $\langle t \rangle$ in each channel needs to be measured.

The determination of the mean decay time is performed through a fit to the decay time distribution of the signal candidates. Candidates with negative measured decay times are included in the fit to have a better handle on the acceptance and the resolution function. The measured decay time distribution is modelled by a decreasing exponential function, with mean lifetime τ , convolved with a double Gaussian resolution function and multiplied with an acceptance function of the form

$$A(t) = 1 - a e^{-(t/(b\tau))^2}, \quad (9)$$

where a and b are acceptance parameters. The fit model is motivated by simulation studies. The values for the fraction and width of the second Gaussian and the acceptance parameter b are taken from the simulation and fixed in the fit. The role of the acceptance parametrisation is to allow a fit to the distribution such that the resolution effect can be removed and the true decay time, which appears in Eq. (8), can be evaluated. The observed decay time distributions with the fit result superimposed are shown in Fig. 4.

The decay time resolutions obtained from the lifetime fit (taken as the width of the first Gaussian function) are 63.3 ± 0.3 fs for $D^0 \rightarrow K^- K^+$ and 58.3 ± 0.4 fs for $D^0 \rightarrow \pi^- \pi^+$, which are about 10% larger than expected from simulations. The main systematic uncertainties come from the uncertainty in the acceptance function and from backgrounds. Using the world average of the D^0 lifetime, $\tau(D^0) = 410.1 \pm 1.5$ fs, the difference and average of the mean decay times relative to $\tau(D^0)$ are found to be

$$\Delta \langle t \rangle / \tau(D^0) = 0.018 \pm 0.002(\text{stat}) \pm 0.007(\text{syst}), \quad (10)$$

$$\langle \bar{t} \rangle / \tau(D^0) = 1.062 \pm 0.001(\text{stat}) \pm 0.003(\text{syst}), \quad (11)$$

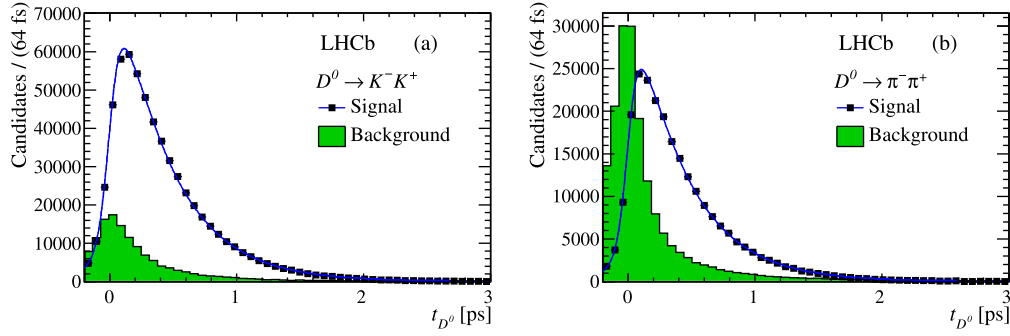


Fig. 4. Decay time distribution for signal candidates (solid points) with the result from the fit overlaid for (a) $D^0 \rightarrow K^- K^+$ and (b) $D^0 \rightarrow \pi^- \pi^+$ decays. The distribution for background candidates scaled to a ± 34 MeV/ c^2 window around the nominal D^0 mass is shown in the shaded (green in the web version) region. The distributions for signal and background candidates are obtained using the *sPlot* method.

where the uncertainty in $\tau(D^0)$ is included as a systematic uncertainty. Note that $\langle \bar{t} \rangle$ is not a measurement of the D^0 effective lifetime (i.e., the lifetime measured with a single exponential fit), since this number contains effects from the LHCb acceptance. The small value of $\Delta(t)$ implies that the measured value of ΔA_{CP} is equal to the difference in direct CP violation, i.e., $\Delta A_{CP} = \Delta a_{CP}^{\text{dir}}$ with negligible corrections.

7. Systematic uncertainties

The contributions to the systematic uncertainty on ΔA_{CP} are described below.

- Difference in b -hadron mixture.** Due to the momentum requirements in the trigger and selection, the relative contribution from B^0 and B^+ decays (the contribution from b -baryon and B_s^0 decays can be neglected) can be different between the $D^0 \rightarrow K^- K^+$ and $D^0 \rightarrow \pi^- \pi^+$ modes. In combination with a different effective production asymmetry for candidates from B^0 and B^+ mesons (the production asymmetry from B^0 mesons is diluted due to B^0 mixing) this could lead to a non-vanishing bias in ΔA_{CP} . Assuming isospin symmetry, the production cross-sections for B^0 and B^+ mesons are expected to be equal. Therefore, the ratio between B^0 and B^+ decays is primarily determined by their branching fractions to the $D^0 \mu X$ final state. Using the inclusive branching fractions [24], $B^{+0} \rightarrow \bar{D}^0 X$, the B^0 fraction is expected to be $f(B^0) = (37.5 \pm 2.9)\%$. From the simulation the difference in the B^0 fraction due to the difference in selection efficiencies is found to be at maximum 1%. Further assuming a B^+ production asymmetry of 1.0% [25] and assuming no B^0 production asymmetry, the difference in the effective production asymmetry between the two modes is $\sim 0.02\%$.
- Difference in B decay time acceptance.** A difference between the $D^0 \rightarrow K^- K^+$ and $D^0 \rightarrow \pi^- \pi^+$ modes in the B decay time acceptance, in combination with B^0 mixing, changes the effective B production asymmetry. Its effect is estimated from integrating the expected B decay time distributions at different starting values, such that the mean lifetime ratio corresponds to the observed B decay length difference ($\sim 5\%$) in the two modes. Using the estimated B^0 fraction and assuming a 1.0% production asymmetry, the effect on ΔA_{CP} is found to be 0.02%.
- Effect of the weighting procedure.** After weighting the D^0 distributions in p_T and η , only small differences remain in the muon kinematic distributions. In order to estimate the systematic uncertainty from the B production and detection asymmetry due to residual differences in the muon kinematic distributions, an additional weight is applied according to the muon (p_T, η) and the azimuthal angle ϕ . The value of ΔA_{CP} changes by 0.05%.
- Difference in mistag asymmetry.** The difference in the mistag rate between positive and negative tags contributes to the measured raw asymmetry. The mistag difference using $D^0 \rightarrow K^- \pi^+$ decays is measured to be $\Delta\omega = (0.006 \pm 0.021)\%$ (see Section 5.2). In case $\Delta\omega$ is different for $D^0 \rightarrow K^- K^+$ and $D^0 \rightarrow \pi^- \pi^+$ there can be a small effect from the mistag asymmetry. A systematic uncertainty of 0.02% is assigned, coming from the uncertainty on $\Delta\omega$.
- Effect of different fit models.** A possible asymmetry in the background from false D^0 combinations is accounted for in the fit to the D^0 mass distribution. Different models can change the fraction between signal and background and therefore change the observed asymmetry. The baseline model is modified by either using a single Gaussian function for the signal, a single Gaussian plus a Crystal Ball function for the signal, a first- or second-order polynomial for the background, by leaving the asymmetry in the reflection free, or by modifying the fit range for $D^0 \rightarrow \pi^- \pi^+$ to exclude the reflection peak. The largest variation changes the value of ΔA_{CP} by 0.035%. As another check, the asymmetry is determined without any fit by counting the number of positively- and negatively-tagged events in the signal window and subtracting the corresponding numbers in the sideband windows. The sideband windows are defined as $[\mu_{\text{sig}} - 48 \text{ MeV}/c^2, \mu_{\text{sig}} - 34 \text{ MeV}/c^2]$ and $[\mu_{\text{sig}} + 34 \text{ MeV}/c^2, \mu_{\text{sig}} + 48 \text{ MeV}/c^2]$, and the signal window as $[\mu_{\text{sig}} - 14 \text{ MeV}/c^2, \mu_{\text{sig}} + 14 \text{ MeV}/c^2]$, where μ_{sig} is the mean of the signal distribution. This method changes the value of ΔA_{CP} by 0.05%, which is taken as a systematic uncertainty.
- Low-lifetime background in $D^0 \rightarrow \pi^- \pi^+$.** As can be seen in Fig. 4, there is more background around $t = 0$ in the $D^0 \rightarrow \pi^- \pi^+$ channel compared to the $D^0 \rightarrow K^- K^+$ channel. If this background exhibits a non-flat or peaking structure this could bias the measurement of ΔA_{CP} . When including the negative lifetime events the value of ΔA_{CP} changes by 0.11%. This shift is taken as a systematic uncertainty.
- Λ_c^+ background in $D^0 \rightarrow K^- K^+$.** A non-negligible fraction of the background in the $D^0 \rightarrow K^- K^+$ mode originates from partial reconstruction of $\Lambda_c^+ \rightarrow p K^- \pi^+$ decays, where the proton is misidentified as a kaon. Most of these Λ_c^+ decays are expected to come from semileptonic Λ_b^0 decays. From exclusively reconstructed Λ_c^+ decays the shape of the background is observed to be linear in the $K^- K^+$ invariant mass distribution. The influence of such a linear background on the fit model is tested by generating many pseudo-experiments. With an asymmetry in the Λ_c^+ background of 3%, which is a conser-

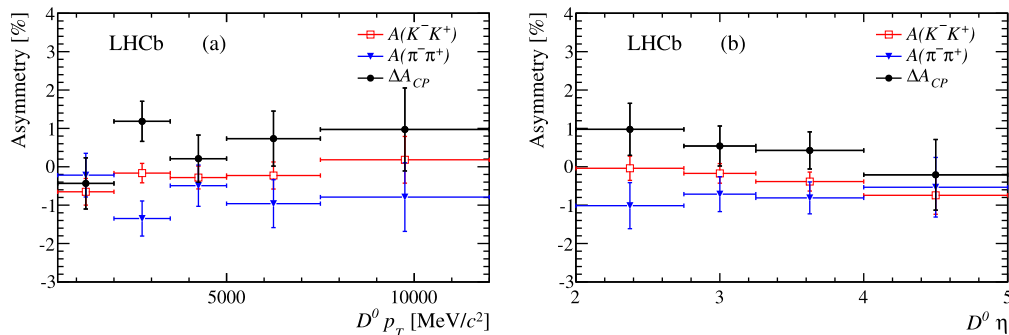


Fig. 5. Raw asymmetries and ΔA_{CP} as a function of (a) p_T and (b) η of the D^0 meson. No weighting is applied.

Table 3

Contributions to the systematic uncertainty of ΔA_{CP} .

Source of uncertainty	Absolute uncertainty
<i>Production asymmetry:</i>	
Difference in b -hadron mixture	0.02%
Difference in B decay time acceptance	0.02%
<i>Production and detection asymmetry:</i>	
Different weighting	0.05%
<i>Background from real D^0 mesons:</i>	
Mistag asymmetry	0.02%
<i>Background from fake D^0 mesons:</i>	
D^0 mass fit model	0.05%
Low-lifetime background in $D^0 \rightarrow \pi^- \pi^+$	0.11%
Λ_c^+ background in $D^0 \rightarrow K^- K^+$	0.03%
<i>Quadratic sum</i>	0.14%

vative upper bound for the asymmetry observed in the exclusively reconstructed Λ_c^+ decays, a small bias of 0.03% is seen in the measured asymmetry. This bias is taken as a systematic uncertainty.

The systematic uncertainties are summarised in Table 3. The effects from higher-order corrections to Eq. (3) and of the uncertainty in the average mistag rate are found to be negligible. The overall systematic uncertainty on ΔA_{CP} , obtained by adding the individual contributions in quadrature, is 0.14%.

8. Cross-checks

Many cross-checks have been performed to verify the stability of the result. In particular, the raw asymmetries and ΔA_{CP} are found to be stable when applying fiducial cuts in the two-dimensional space of the muon momentum and its horizontal component, when comparing different trigger decisions and when applying tighter particle identification requirements on the D^0 daughters or on the muons. The stability of the raw asymmetries and ΔA_{CP} is also investigated as a function of all possible reconstructed quantities, for instance the D^0 decay time, the b -hadron flight distance, the reconstructed D^0 -muon mass, the angle between the muon and D^0 daughters, and the (transverse) momenta and pseudorapidity of the muon and D^0 meson. No significant dependence is observed in any of these variables. For example, Fig. 5 shows ΔA_{CP} and the raw asymmetries in the $D^0 \rightarrow K^- K^+$ and $D^0 \rightarrow \pi^- \pi^+$ modes as a function of p_T and η of the D^0 meson, which are the variables that are used in the weighting procedure. To check for a possible time dependence of the detection asymmetry the data taking period is divided into six parts of roughly equal integrated luminosity. The six parts are separated by periods without beam and changes in the magnet polarity. No significant variation of the raw asymmetries is observed.

9. Conclusion

The difference in CP asymmetries between the $D^0 \rightarrow K^- K^+$ and $D^0 \rightarrow \pi^- \pi^+$ modes is measured using D^0 mesons produced in semileptonic B decays and is found to be

$$\Delta A_{CP} = (0.49 \pm 0.30 \text{ (stat)} \pm 0.14 \text{ (syst)})\%.$$

This result takes into account the muon mistag probability and differences in the kinematic distributions of $D^0 \rightarrow K^- K^+$ and $D^0 \rightarrow \pi^- \pi^+$ decays. When neglecting indirect CP violation the difference between this result and the previous published LHCb result using prompt D^0 decays [5] is 3.2 standard deviations, assuming that the uncertainties have a Gaussian distribution. The discrepancy, however, is reduced to 2.2 standard deviations comparing to a preliminary update of the previous result [26]. This result does not confirm the evidence for direct CP violation in the charm sector.

Acknowledgements

We express our gratitude to our colleagues in the CERN accelerator departments for the excellent performance of the LHC. We thank the technical and administrative staff at the LHCb institutes. We acknowledge support from CERN and from the national agencies: CAPES, CNPq, FAPERJ and FINEP (Brazil); NSFC (China); CNRS/IN2P3 and Region Auvergne (France); BMBF, DFG, HGF and MPG (Germany); SFI (Ireland); INFN (Italy); FOM and NWO (The Netherlands); SCSR (Poland); ANCS/IFA (Romania); MinES, Rosatom, RFBR and NRC “Kurchatov Institute” (Russia); MinEco, XuntaGal and GENCAT (Spain); SNSF and SER (Switzerland); NAS Ukraine (Ukraine); STFC (United Kingdom); NSF (USA). We also acknowledge the support received from the ERC under FP7. The Tier1 computing centres are supported by IN2P3 (France), KIT and BMBF (Germany), INFN (Italy), NWO and SURF (The Netherlands), PIC (Spain), GridPP (United Kingdom). We are thankful for the computing resources put at our disposal by Yandex LLC (Russia), as well as to the communities behind the multiple open source software packages that we depend on.

Open access

This article is published Open Access at sciencedirect.com. It is distributed under the terms of the Creative Commons Attribution License 3.0, which permits unrestricted use, distribution, and reproduction in any medium, provided the original authors and source are credited.

References

- [1] N. Cabibbo, *Phys. Rev. Lett.* **10** (1963) 531.

- [2] M. Kobayashi, T. Maskawa, Prog. Theor. Phys. 49 (1973) 652.
- [3] S. Bianco, F. Fabbri, D. Benson, I. Bigi, Riv. Nuovo Cim. 26 (7) (2003) 1, arXiv:hep-ex/0309021.
- [4] Y. Grossman, A.L. Kagan, Y. Nir, Phys. Rev. D 75 (2007) 036008, arXiv:hep-ph/0609178.
- [5] LHCb Collaboration, R. Aaij, et al., Phys. Rev. Lett. 108 (2012) 111602, arXiv:1112.0938.
- [6] LHCb Collaboration, R. Aaij, et al., Eur. Phys. J. C 73 (2013) 2373, <http://dx.doi.org/10.1140/epjc/s10052-013-2373-2>, arXiv:1208.3355.
- [7] CDF Collaboration, T. Aaltonen, et al., Phys. Rev. Lett. 109 (2012) 111801, arXiv:1207.2158.
- [8] B. Ko, Direct CP violation in charm at Belle, arXiv:1212.1975.
- [9] Heavy Flavor Averaging Group, Y. Amhis, et al., Averages of b-hadron, c-hadron, and tau-lepton properties as of early 2012, arXiv:1207.1158, updated averages and plots available from <http://www.slac.stanford.edu/xorg/hfag/>.
- [10] BaBar Collaboration, B. Aubert, et al., Phys. Rev. Lett. 100 (2008) 061803, arXiv:0709.2715.
- [11] LHCb Collaboration, A.A. Alves Jr., et al., JINST 3 (2008) S08005.
- [12] M. Adinolfi, et al., Performance of the LHCb RICH detector at the LHC, arXiv:1211.6759, Eur. Phys. J. C (2013), in press.
- [13] R. Aaij, et al., JINST 8 (2013) P04022, <http://dx.doi.org/10.1088/1748-0221/8/04/P04022>, arXiv:1211.3055.
- [14] T. Sjöstrand, S. Mrenna, P. Skands, JHEP 0605 (2006) 026, arXiv:hep-ph/0603175.
- [15] I. Belyaev, et al., in: Nuclear Science Symposium Conference Record (NSS/MIC), IEEE, 2010, p. 1155.
- [16] D.J. Lange, Nucl. Instrum. Meth. A 462 (2001) 152.
- [17] P. Golonka, Z. Was, Eur. Phys. J. C 45 (2006) 97, arXiv:hep-ph/0506026.
- [18] GEANT4 Collaboration, J. Allison, et al., IEEE Trans. Nucl. Sci. 53 (2006) 270; GEANT4 Collaboration, S. Agostinelli, et al., Nucl. Instrum. Meth. A 506 (2003) 250.
- [19] M. Clemencic, et al., J. Phys.: Conf. Ser. 331 (2011) 032023.
- [20] M. Pivk, F.R. Le Diberder, Nucl. Instrum. Meth. A 555 (2005) 356, arXiv:physics/0402083.
- [21] LHCb Collaboration, R. Aaij, et al., Phys. Rev. Lett. 110 (2013) 101802, arXiv:1211.1230.
- [22] LHCb Collaboration, R. Aaij, et al., JHEP 1204 (2012) 129, arXiv:1112.4698.
- [23] M. Gersabeck, et al., J. Phys. G 39 (2012) 045005, arXiv:1111.6515.
- [24] Particle Data Group, J. Beringer, et al., Phys. Rev. D 86 (2012) 010001.
- [25] LHCb Collaboration, R. Aaij, et al., Phys. Rev. Lett. 108 (2012) 201601, arXiv:1202.6251.
- [26] LHCb Collaboration, A search for time-integrated CP violation in $D^0 \rightarrow K^- K^+$ and $D^0 \rightarrow \pi^- \pi^+$ decays, LHCb-CONF-2013-003.

LHCb Collaboration

R. Aaij⁴⁰, C. Abellan Beteta^{35,n}, B. Adeva³⁶, M. Adinolfi⁴⁵, C. Adrover⁶, A. Affolder⁵¹, Z. Ajaltouni⁵, J. Albrecht⁹, F. Alessio³⁷, M. Alexander⁵⁰, S. Ali⁴⁰, G. Alkhazov²⁹, P. Alvarez Cartelle³⁶, A.A. Alves Jr.^{24,37}, S. Amato², S. Amerio²¹, Y. Amhis⁷, L. Anderlini^{17,f}, J. Anderson³⁹, R. Andreassen⁵⁹, R.B. Appleby⁵³, O. Aquines Gutierrez¹⁰, F. Archilli¹⁸, A. Artamonov³⁴, M. Artuso⁵⁶, E. Aslanides⁶, G. Auremma^{24,m}, S. Bachmann¹¹, J.J. Back⁴⁷, C. Baesso⁵⁷, V. Balagura³⁰, W. Baldini¹⁶, R.J. Barlow⁵³, C. Barschel³⁷, S. Barsuk⁷, W. Barter⁴⁶, Th. Bauer⁴⁰, A. Bay³⁸, J. Beddow⁵⁰, F. Bedeschi²², I. Bediaga¹, S. Belogurov³⁰, K. Belous³⁴, I. Belyaev³⁰, E. Ben-Haim⁸, M. Benayoun⁸, G. Bencivenni¹⁸, S. Benson⁴⁹, J. Benton⁴⁵, A. Berezhnoy³¹, R. Bernet³⁹, M.-O. Bettler⁴⁶, M. van Beuzekom⁴⁰, A. Bien¹¹, S. Bifani¹², T. Bird⁵³, A. Bizzeti^{17,h}, P.M. Bjørnstad⁵³, T. Blake³⁷, F. Blanc³⁸, J. Blouw¹¹, S. Blusk⁵⁶, V. Bocci²⁴, A. Bondar³³, N. Bondar²⁹, W. Bonivento¹⁵, S. Borghi⁵³, A. Borgia⁵⁶, T.J.V. Bowcock⁵¹, E. Bowen³⁹, C. Bozzi¹⁶, T. Brambach⁹, J. van den Brand⁴¹, J. Bressieux³⁸, D. Brett⁵³, M. Britsch¹⁰, T. Britton⁵⁶, N.H. Brook⁴⁵, H. Brown⁵¹, I. Burducea²⁸, A. Bursche³⁹, G. Busetto^{21,q}, J. Buytaert³⁷, S. Cadettu¹⁵, O. Callot⁷, M. Calvi^{20,j}, M. Calvo Gomez^{35,n}, A. Camboni³⁵, P. Campana^{18,37}, D. Campora Perez³⁷, A. Carbone^{14,c}, G. Carboni^{23,k}, R. Cardinale^{19,i}, A. Cardini¹⁵, H. Carranza-Mejia⁴⁹, L. Carson⁵², K. Carvalho Akiba², G. Casse⁵¹, M. Cattaneo³⁷, Ch. Cauet⁹, M. Charles⁵⁴, Ph. Charpentier³⁷, P. Chen^{3,38}, N. Chiapolini³⁹, M. Chrzaszcz²⁵, K. Ciba³⁷, X. Cid Vidal³⁷, G. Ciezarek⁵², P.E.L. Clarke⁴⁹, M. Clemencic³⁷, H.V. Cliff⁴⁶, J. Closier³⁷, C. Coca²⁸, V. Coco⁴⁰, J. Cogan⁶, E. Cogneras⁵, P. Collins³⁷, A. Comerma-Montells³⁵, A. Contu¹⁵, A. Cook⁴⁵, M. Coombes⁴⁵, S. Coquereau⁸, G. Corti³⁷, B. Couturier³⁷, G.A. Cowan⁴⁹, D. Craik⁴⁷, S. Cunliffe⁵², R. Currie⁴⁹, C. D'Ambrosio³⁷, P. David⁸, P.N.Y. David⁴⁰, I. De Bonis⁴, K. De Bruyn⁴⁰, S. De Capua⁵³, M. De Cian³⁹, J.M. De Miranda¹, L. De Paula², W. De Silva⁵⁹, P. De Simone¹⁸, D. Decamp⁴, M. Deckenhoff⁹, L. Del Buono⁸, D. Derkach¹⁴, O. Deschamps⁵, F. Dettori⁴¹, H. Dijkstra³⁷, M. Dogaru²⁸, S. Donleavy⁵¹, F. Dordei¹¹, A. Dosil Suárez³⁶, D. Dossett⁴⁷, A. Dovbnya⁴², F. Dupertuis³⁸, R. Dzhelyadin³⁴, A. Dziurda²⁵, A. Dzyuba²⁹, S. Easo^{48,37}, U. Egede⁵², V. Egorychev³⁰, S. Eidelman³³, D. van Eijk⁴⁰, S. Eisenhardt⁴⁹, U. Eitschberger⁹, R. Ekelhof⁹, L. Eklund^{50,37}, I. El Rifai⁵, Ch. Elsasser³⁹, D. Elsby⁴⁴, A. Falabella^{14,e}, C. Färber¹¹, G. Fardell⁴⁹, C. Farinelli⁴⁰, S. Farry¹², V. Fave³⁸, D. Ferguson⁴⁹, V. Fernandez Albor³⁶, F. Ferreira Rodrigues¹, M. Ferro-Luzzi³⁷, S. Filippov³², M. Fiore¹⁶, C. Fitzpatrick³⁷, M. Fontana¹⁰, F. Fontanelli^{19,i}, R. Forty³⁷, O. Francisco², M. Frank³⁷, C. Frei³⁷, M. Frosini^{17,f}, S. Furcas²⁰, E. Furfaro²³, A. Gallas Torreira³⁶, D. Galli^{14,c}, M. Gandelman², P. Gandini⁵⁶, Y. Gao³, J. Garofoli⁵⁶, P. Garosi⁵³, J. Garra Tico⁴⁶, L. Garrido³⁵, C. Gaspar³⁷, R. Gauld⁵⁴, E. Gersabeck¹¹, M. Gersabeck⁵³, T. Gershon^{47,37}, Ph. Ghez⁴, V. Gibson⁴⁶, V.V. Gligorov³⁷, C. Göbel⁵⁷, D. Golubkov³⁰, A. Golutvin^{52,30,37}, A. Gomes², H. Gordon⁵⁴, M. Grabalosa Gándara⁵, R. Graciani Diaz³⁵, L.A. Granado Cardoso³⁷, E. Graugés³⁵, G. Graziani¹⁷, A. Grecu²⁸, E. Greening⁵⁴, S. Gregson⁴⁶, O. Grünberg⁵⁸, B. Gui⁵⁶, E. Gushchin³², Yu. Guz^{34,37}, T. Gys³⁷, C. Hadjivasiliou⁵⁶, G. Haefeli³⁸, C. Haen³⁷, S.C. Haines⁴⁶, S. Hall⁵², T. Hampson⁴⁵, S. Hansmann-Menzemer¹¹, N. Harnew⁵⁴, S.T. Harnew⁴⁵, J. Harrison⁵³, T. Hartmann⁵⁸, J. He³⁷,

V. Heijne⁴⁰, K. Hennessy⁵¹, P. Henrard⁵, J.A. Hernando Morata³⁶, E. van Herwijnen³⁷, E. Hicks⁵¹, D. Hill⁵⁴, M. Hoballah⁵, C. Hombach⁵³, P. Hopchev⁴, W. Hulsbergen⁴⁰, P. Hunt⁵⁴, T. Huse⁵¹, N. Hussain⁵⁴, D. Hutchcroft⁵¹, D. Hynds⁵⁰, V. Iakovenko⁴³, M. Idzik²⁶, P. Ilten¹², R. Jacobsson³⁷, A. Jaeger¹¹, E. Jans⁴⁰, P. Jaton³⁸, F. Jing³, M. John⁵⁴, D. Johnson⁵⁴, C.R. Jones⁴⁶, B. Jost³⁷, M. Kabbalo⁹, S. Kandybei⁴², M. Karacson³⁷, T.M. Karbach³⁷, I.R. Kenyon⁴⁴, U. Kerzel³⁷, T. Ketel⁴¹, A. Keune³⁸, B. Khanji²⁰, O. Kochebina⁷, I. Komarov³⁸, R.F. Koopman⁴¹, P. Koppenburg⁴⁰, M. Korolev³¹, A. Kozlinskiy⁴⁰, L. Kravchuk³², K. Kreplin¹¹, M. Kreps⁴⁷, G. Krocker¹¹, P. Krokovny³³, F. Kruse⁹, M. Kucharczyk^{20,25,j}, V. Kudryavtsev³³, T. Kvaratskheliya^{30,37}, V.N. La Thi³⁸, D. Lacarrere³⁷, G. Lafferty⁵³, A. Lai¹⁵, D. Lambert⁴⁹, R.W. Lambert⁴¹, E. Lanciotti³⁷, G. Lanfranchi^{18,37}, C. Langenbruch³⁷, T. Latham⁴⁷, C. Lazzeroni⁴⁴, R. Le Gac⁶, J. van Leerdam⁴⁰, J.-P. Lees⁴, R. Lefèvre⁵, A. Leflat³¹, J. Lefrançois⁷, S. Leo²², O. Leroy⁶, B. Leverington¹¹, Y. Li³, L. Li Gioi⁵, M. Liles⁵¹, R. Lindner³⁷, C. Linn¹¹, B. Liu³, G. Liu³⁷, S. Lohn³⁷, I. Longstaff⁵⁰, J.H. Lopes², E. Lopez Asamar³⁵, N. Lopez-March³⁸, H. Lu³, D. Lucchesi^{21,q}, J. Luisier³⁸, H. Luo⁴⁹, F. Machefert⁷, I.V. Machikhiliyan^{4,30}, F. Maciuc²⁸, O. Maev^{29,37}, S. Malde⁵⁴, G. Manca^{15,d}, G. Mancinelli⁶, U. Marconi¹⁴, R. Märki³⁸, J. Marks¹¹, G. Martellotti²⁴, A. Martens⁸, L. Martin⁵⁴, A. Martín Sánchez⁷, M. Martinelli⁴⁰, D. Martinez Santos⁴¹, D. Martins Tostes², A. Massafferri¹, R. Matev³⁷, Z. Mathe³⁷, C. Matteuzzi²⁰, E. Maurice⁶, A. Mazurov^{16,32,37,e}, J. McCarthy⁴⁴, R. McNulty¹², A. McNab⁵³, B. Meadows^{59,54}, F. Meier⁹, M. Meissner¹¹, M. Merk⁴⁰, D.A. Milanes⁸, M.-N. Minard⁴, J. Molina Rodriguez⁵⁷, S. Monteil⁵, D. Moran⁵³, P. Morawski²⁵, M.J. Morello^{22,s}, R. Mountain⁵⁶, I. Mous⁴⁰, F. Muheim⁴⁹, K. Müller³⁹, R. Muresan²⁸, B. Muryn²⁶, B. Muster³⁸, P. Naik⁴⁵, T. Nakada³⁸, R. Nandakumar⁴⁸, I. Nasteva¹, M. Needham⁴⁹, N. Neufeld³⁷, A.D. Nguyen³⁸, T.D. Nguyen³⁸, C. Nguyen-Mau^{38,p}, M. Nicol⁷, V. Niess⁵, R. Niet⁹, N. Nikitin³¹, T. Nikodem¹¹, A. Nomerotski⁵⁴, A. Novoselov³⁴, A. Oblakowska-Mucha²⁶, V. Obraztsov³⁴, S. Oggero⁴⁰, S. Ogilvy⁵⁰, O. Okhrimenko⁴³, R. Oldeman^{15,d}, M. Orlandea²⁸, J.M. Otalora Goicochea², P. Owen⁵², A. Oyanguren^{35,o}, B.K. Pal⁵⁶, A. Palano^{13,b}, M. Palutan¹⁸, J. Panman³⁷, A. Papanestis⁴⁸, M. Pappagallo⁵⁰, C. Parkes⁵³, C.J. Parkinson⁵², G. Passaleva¹⁷, G.D. Patel⁵¹, M. Patel⁵², G.N. Patrick⁴⁸, C. Patrignani^{19,i}, C. Pavel-Nicorescu²⁸, A. Pazos Alvarez³⁶, A. Pellegrino⁴⁰, G. Penso^{24,l}, M. Pepe Altarelli³⁷, S. Perazzini^{14,c}, D.L. Perego^{20,j}, E. Perez Trigo³⁶, A. Pérez-Calero Yzquierdo³⁵, P. Perret⁵, M. Perrin-Terrin⁶, G. Pessina²⁰, K. Petridis⁵², A. Petrolini^{19,i}, A. Phan⁵⁶, E. Picatoste Olloqui³⁵, B. Pietrzyk⁴, T. Pilař⁴⁷, D. Pinci²⁴, S. Playfer⁴⁹, M. Plo Casasus³⁶, F. Polci⁸, G. Polok²⁵, A. Poluektov^{47,33}, E. Polycarpo², D. Popov¹⁰, B. Popovici²⁸, C. Potterat³⁵, A. Powell⁵⁴, J. Prisciandaro³⁸, V. Pugatch⁴³, A. Puig Navarro³⁸, G. Punzi^{22,r}, W. Qian⁴, J.H. Rademacker⁴⁵, B. Rakotomiaramanana³⁸, M.S. Rangel², I. Raniuk⁴², N. Rauschmayr³⁷, G. Raven⁴¹, S. Redford⁵⁴, M.M. Reid⁴⁷, A.C. dos Reis¹, S. Ricciardi⁴⁸, A. Richards⁵², K. Rinnert⁵¹, V. Rives Molina³⁵, D.A. Roa Romero⁵, P. Robbe⁷, E. Rodrigues⁵³, P. Rodriguez Perez³⁶, S. Roiser³⁷, V. Romanovsky³⁴, A. Romero Vidal³⁶, J. Rouvinet³⁸, T. Ruf³⁷, F. Ruffini²², H. Ruiz³⁵, P. Ruiz Valls^{35,o}, G. Sabatino^{24,k}, J.J. Saborido Silva³⁶, N. Sagidova²⁹, P. Sail⁵⁰, B. Saitta^{15,d}, C. Salzmann³⁹, B. Sanmartin Sedes³⁶, M. Sannino^{19,i}, R. Santacesaria²⁴, C. Santamarina Rios³⁶, E. Santovetti^{23,k}, M. Sapunov⁶, A. Sarti^{18,l}, C. Satriano^{24,m}, A. Satta²³, M. Savrie^{16,e}, D. Savrina^{30,31}, P. Schaack⁵², M. Schiller⁴¹, H. Schindler³⁷, M. Schlupp⁹, M. Schmelling¹⁰, B. Schmidt³⁷, O. Schneider³⁸, A. Schopper³⁷, M.-H. Schune⁷, R. Schwemmer³⁷, B. Sciascia¹⁸, A. Sciubba²⁴, M. Seco³⁶, A. Semennikov³⁰, K. Senderowska²⁶, I. Sepp⁵², N. Serra³⁹, J. Serrano⁶, P. Seyfert¹¹, M. Shapkin³⁴, I. Shapoval^{16,42}, P. Shatalov³⁰, Y. Shcheglov²⁹, T. Shears^{51,37}, L. Shekhtman³³, O. Shevchenko⁴², V. Shevchenko³⁰, A. Shires⁵², R. Silva Coutinho⁴⁷, T. Skwarnicki⁵⁶, N.A. Smith⁵¹, E. Smith^{54,48}, M. Smith⁵³, M.D. Sokoloff⁵⁹, F.J.P. Soler⁵⁰, F. Soomro¹⁸, D. Souza⁴⁵, B. Souza De Paula², B. Spaan⁹, A. Sparkes⁴⁹, P. Spradlin⁵⁰, F. Stagni³⁷, S. Stahl¹¹, O. Steinkamp³⁹, S. Stoica²⁸, S. Stone⁵⁶, B. Storaci³⁹, M. Straticiu²⁸, U. Straumann³⁹, V.K. Subbiah³⁷, S. Swientek⁹, V. Syropoulos⁴¹, M. Szczekowski²⁷, P. Szczypka^{38,37}, T. Szumlak²⁶, S. T'Jampens⁴, M. Teklishyn⁷, E. Teodorescu²⁸, F. Teubert³⁷, C. Thomas⁵⁴, E. Thomas³⁷, J. van Tilburg^{11,*}, V. Tisserand⁴, M. Tobin³⁸, S. Tolk⁴¹, S. Topp-Joergensen⁵⁴, N. Torr⁵⁴, E. Tournefier^{4,52}, S. Tourneur³⁸, M.T. Tran³⁸, M. Tresch³⁹, A. Tsaregorodtsev⁶, P. Tsopelas⁴⁰, N. Tuning⁴⁰, M. Ubeda Garcia³⁷, A. Ukleja²⁷, D. Urner⁵³, U. Uwer¹¹, V. Vagnoni¹⁴, G. Valenti¹⁴, R. Vazquez Gomez³⁵, P. Vazquez Regueiro³⁶, S. Vecchi¹⁶, J.J. Velthuis⁴⁵, M. Veltri^{17,g}, G. Veneziano³⁸, M. Vesterinen³⁷, B. Viaud⁷, D. Vieira², X. Vilasis-Cardona^{35,n}, A. Vollhardt³⁹, D. Volyansky¹⁰, D. Voong⁴⁵,

A. Vorobyev²⁹, V. Vorobyev³³, C. Voß⁵⁸, H. Voss¹⁰, R. Waldi⁵⁸, R. Wallace¹², S. Wandernoth¹¹, J. Wang⁵⁶, D.R. Ward⁴⁶, N.K. Watson⁴⁴, A.D. Webber⁵³, D. Websdale⁵², M. Whitehead⁴⁷, J. Wicht³⁷, J. Wiechczynski²⁵, D. Wiedner¹¹, L. Wiggers⁴⁰, G. Wilkinson⁵⁴, M.P. Williams^{47,48}, M. Williams⁵⁵, F.F. Wilson⁴⁸, J. Wishahi⁹, M. Witek²⁵, S.A. Wotton⁴⁶, S. Wright⁴⁶, S. Wu³, K. Wyllie³⁷, Y. Xie^{49,37}, F. Xing⁵⁴, Z. Xing⁵⁶, Z. Yang³, R. Young⁴⁹, X. Yuan³, O. Yushchenko³⁴, M. Zangoli¹⁴, M. Zavertyaev^{10,a}, F. Zhang³, L. Zhang⁵⁶, W.C. Zhang¹², Y. Zhang³, A. Zhelezov¹¹, A. Zhokhov³⁰, L. Zhong³, A. Zvyagin³⁷

¹ Centro Brasileiro de Pesquisas Físicas (CBPF), Rio de Janeiro, Brazil

² Universidade Federal do Rio de Janeiro (UFRJ), Rio de Janeiro, Brazil

³ Center for High Energy Physics, Tsinghua University, Beijing, China

⁴ LAPP, Université de Savoie, CNRS/IN2P3, Annecy-Le-Vieux, France

⁵ Clermont Université, Université Blaise Pascal, CNRS/IN2P3, LPC, Clermont-Ferrand, France

⁶ CPPM, Aix-Marseille Université, CNRS/IN2P3, Marseille, France

⁷ LAL, Université Paris-Sud, CNRS/IN2P3, Orsay, France

⁸ LPNHE, Université Pierre et Marie Curie, Université Paris Diderot, CNRS/IN2P3, Paris, France

⁹ Fakultät Physik, Technische Universität Dortmund, Dortmund, Germany

¹⁰ Max-Planck-Institut für Kernphysik (MPIK), Heidelberg, Germany

¹¹ Physikalisches Institut, Ruprecht-Karls-Universität Heidelberg, Heidelberg, Germany

¹² School of Physics, University College Dublin, Dublin, Ireland

¹³ Sezione INFN di Bari, Bari, Italy

¹⁴ Sezione INFN di Bologna, Bologna, Italy

¹⁵ Sezione INFN di Cagliari, Cagliari, Italy

¹⁶ Sezione INFN di Ferrara, Ferrara, Italy

¹⁷ Sezione INFN di Firenze, Firenze, Italy

¹⁸ Laboratori Nazionali dell'INFN di Frascati, Frascati, Italy

¹⁹ Sezione INFN di Genova, Genova, Italy

²⁰ Sezione INFN di Milano Bicocca, Milano, Italy

²¹ Sezione INFN di Padova, Padova, Italy

²² Sezione INFN di Pisa, Pisa, Italy

²³ Sezione INFN di Roma Tor Vergata, Roma, Italy

²⁴ Sezione INFN di Roma La Sapienza, Roma, Italy

²⁵ Henryk Niewodniczanski Institute of Nuclear Physics Polish Academy of Sciences, Kraków, Poland

²⁶ AGH University of Science and Technology, Kraków, Poland

²⁷ National Center for Nuclear Research (NCBJ), Warsaw, Poland

²⁸ Horia Hulubei National Institute of Physics and Nuclear Engineering, Bucharest-Magurele, Romania

²⁹ Petersburg Nuclear Physics Institute (PNPI), Gatchina, Russia

³⁰ Institute of Theoretical and Experimental Physics (ITEP), Moscow, Russia

³¹ Institute of Nuclear Physics, Moscow State University (SINP MSU), Moscow, Russia

³² Institute for Nuclear Research of the Russian Academy of Sciences (INR RAN), Moscow, Russia

³³ Budker Institute of Nuclear Physics (SB RAS) and Novosibirsk State University, Novosibirsk, Russia

³⁴ Institute for High Energy Physics (IHEP), Protvino, Russia

³⁵ Universitat de Barcelona, Barcelona, Spain

³⁶ Universidad de Santiago de Compostela, Santiago de Compostela, Spain

³⁷ European Organization for Nuclear Research (CERN), Geneva, Switzerland

³⁸ Ecole Polytechnique Fédérale de Lausanne (EPFL), Lausanne, Switzerland

³⁹ Physik-Institut, Universität Zürich, Zürich, Switzerland

⁴⁰ Nikhef National Institute for Subatomic Physics, Amsterdam, The Netherlands

⁴¹ Nikhef National Institute for Subatomic Physics and VU University Amsterdam, Amsterdam, The Netherlands

⁴² NSC Kharkiv Institute of Physics and Technology (NSC KIPT), Kharkiv, Ukraine

⁴³ Institute for Nuclear Research of the National Academy of Sciences (KINR), Kyiv, Ukraine

⁴⁴ University of Birmingham, Birmingham, United Kingdom

⁴⁵ H.H. Wills Physics Laboratory, University of Bristol, Bristol, United Kingdom

⁴⁶ Cavendish Laboratory, University of Cambridge, Cambridge, United Kingdom

⁴⁷ Department of Physics, University of Warwick, Coventry, United Kingdom

⁴⁸ STFC Rutherford Appleton Laboratory, Didcot, United Kingdom

⁴⁹ School of Physics and Astronomy, University of Edinburgh, Edinburgh, United Kingdom

⁵⁰ School of Physics and Astronomy, University of Glasgow, Glasgow, United Kingdom

⁵¹ Oliver Lodge Laboratory, University of Liverpool, Liverpool, United Kingdom

⁵² Imperial College London, London, United Kingdom

⁵³ School of Physics and Astronomy, University of Manchester, Manchester, United Kingdom

⁵⁴ Department of Physics, University of Oxford, Oxford, United Kingdom

⁵⁵ Massachusetts Institute of Technology, Cambridge, MA, United States

⁵⁶ Syracuse University, Syracuse, NY, United States

⁵⁷ Pontificia Universidade Católica do Rio de Janeiro (PUC-Rio), Rio de Janeiro, Brazil[†]

⁵⁸ Institut für Physik, Universität Rostock, Rostock, Germany[‡]

⁵⁹ University of Cincinnati, Cincinnati, OH, United States[‡]

* Corresponding author.

E-mail address: Jeroen.van.Tilburg@cern.ch (J. van Tilburg).

^a P.N. Lebedev Physical Institute, Russian Academy of Science (LPI RAS), Moscow, Russia.

^b Università di Bari, Bari, Italy.

^c Università di Bologna, Bologna, Italy.

^d Università di Cagliari, Cagliari, Italy.

^e Università di Ferrara, Ferrara, Italy.

^f Università di Firenze, Firenze, Italy.

- ^g Università di Urbino, Urbino, Italy.
- ^h Università di Modena e Reggio Emilia, Modena, Italy.
- ⁱ Università di Genova, Genova, Italy.
- ^j Università di Milano Bicocca, Milano, Italy.
- ^k Università di Roma Tor Vergata, Roma, Italy.
- ^l Università di Roma La Sapienza, Roma, Italy.
- ^m Università della Basilicata, Potenza, Italy.
- ⁿ LIFAELS, La Salle, Universitat Ramon Llull, Barcelona, Spain.
- ^o IFIC, Universitat de Valencia-CSIC, Valencia, Spain.
- ^p Hanoi University of Science, Hanoi, Viet Nam.
- ^q Università di Padova, Padova, Italy.
- ^r Università di Pisa, Pisa, Italy.
- ^s Scuola Normale Superiore, Pisa, Italy.
- ^t Associated to: Universidade Federal do Rio de Janeiro (UFRJ), Rio de Janeiro, Brazil.
- ^u Associated to: Physikalisches Institut, Ruprecht-Karls-Universität Heidelberg, Heidelberg, Germany.
- ^v Associated to: Syracuse University, Syracuse, NY, United States.